Telecom InP/InGaAs nano-laser array directly grown on (001) silicon-on-insulator

YU HAN,[1] WAI KIT NG,[2] YING XUE,[1] QIANG LI,[1] KAM SING WONG,[2] AND KEI MAY LAU[1,*]

[1]*Department of Electronic and Computer Engineering, Hong Kong University of Science and Technology, Clear Water Bay, Kowloon, Hong Kong, China*

[2]*Department of Physics and William Mong Institute of Nano Science and Technology, Hong Kong University of Science and Technology, Clear Water Bay, Kowloon, Hong Kong, China*

**Corresponding author: eekmlau@ust.hk*

Received XX Month XXXX; revised XX Month, XXXX; accepted XX Month XXXX; posted XX Month XXXX (Doc. ID XXXXX); published XX Month XXXX

A compact, efficient and monolithically grown III-V laser source provides an attractive alternative to bonding off-chip lasers for Si photonics research. Although recent demonstrations of micro-lasers on (001) Si wafers using thick metamorphic buffers are encouraging, scaling down the laser footprint to nano-scale and operating the nano-lasers at telecom wavelengths remain a significant challenge. Here, we report monolithically integrated in-plane InP/InGaAs nano-laser array on (001) silicon-on-insulator (SOI) platforms with emission wavelengths covering the entire C-band (1.55 μm). Multiple InGaAs quantum wells are embedded in high-quality InP nano-ridges by selective-area growth on patterned (001) SOI. Combined with air-surrounded InP/Si optical cavities, room-temperature operation at multiple telecom bands is obtained by defining different cavity lengths with lithography. The demonstration of telecom-wavelength monolithic nano-lasers on (001) SOI platforms presents an important step towards fully integrated Si photonics circuits.

http://dx.doi.org/10.1364/OL.99.099999

Recent advances in Si based optoelectronic integrated circuits (OEICs) have been underpinned by the development of some key components such as low loss waveguides, high-speed optical modulators and sensitive photo-detectors [1]. However, the final brick, an efficient and scalable on-chip III-V light source, is still missing [2-3]. To bridge the gap between cost-effective electronics and power-efficient photonics, direct hetero-epitaxy of III-V coherent laser sources on Si substrate offers potential lower cost and wider scalability as compared to chip scale bonding approaches [4]. Through buffer engineering, highly efficient electrical injection III-V quantum dot lasers with promising performance has recently been demonstrated [5-7]. Yet scaling device footprint to nano-meter scale is highly sought-after for ultra-low energy consumption and dense integration of Si based OEICs [8-10]. Prevailing approaches using vertically-aligned III-V nanowires, with helical GaAs/InGaAs nano-pillar cavity [11], GaAs/AlGaAs Fabry-Perot cavity [12] and InGaAs/InGaP photonic crystal nano-beam cavity [13], have successfully integrated nano-lasers on (111) Si substrates, which, however, is not easily-made compatible with present Si photonics chips fabricated on the (001) Si platform. In addition, the operation wavelength is restricted to below the E band (< 1460 nm), possibly due to the degrading mode confinement and the exacerbating optical loss at longer wavelengths [14-15]. Recently, well-aligned in-plane III-V distributed-feedback nano-lasers have been incorporated into the CMOS lines using III-V nano-ridges selectively grown on patterned 300-mm (001) Si wafers [16-17]. However, the nano-lasers were grown on bulk Si substrate, and on-chip mode confinement was realized by either suspending the nano-ridges in air or growing large nano-ridge structures from narrow trenches [18]. This configuration makes it challenging to integrate the lasers with other Si-based photonic components such as waveguides, splitters, (de)multiplexers and modulators that are exclusively processed on silicon-on-insulators (SOI). Additionally,

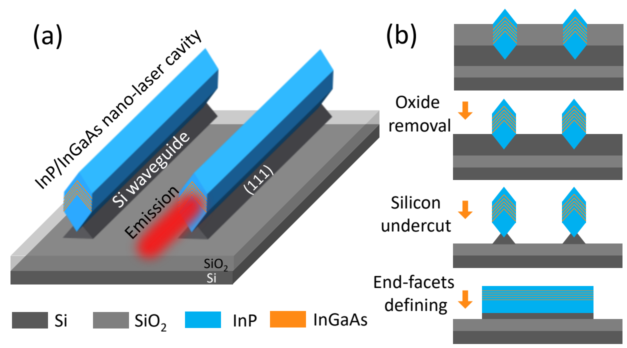

Fig. 1. (a) Schematic of the designed InP/InGaAs nano-laser array grown on SOI substrate. (b) Fabrication process of the InP/InGaAs nano-laser on SOI.

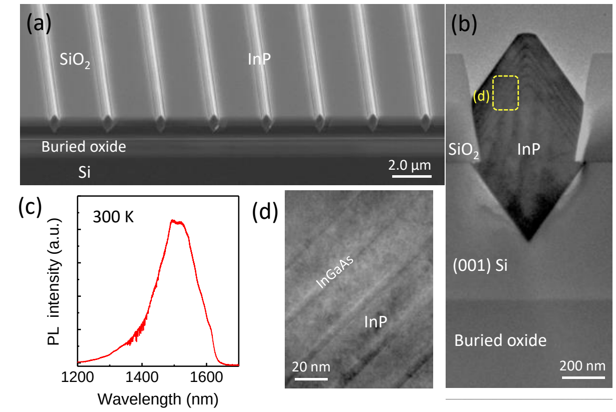

Fig. 2. (a) SEM image of the InP/InGaAs nano-ridge array on (001) SOI. (b) TEM image of one nano-ridge, showing inserted InGaAs ridge QWs and buried oxide layer. (c) Room temperature photoluminescence spectra of the as-grown nano-ridges. (d) Close-up of one side of the InGaAs ridge QWs.

the emission wavelength of these nano-lasers are limited to the O band (< 1360 nm) [17]. For compact and efficient inter/intra-chip data communications, expanding the lasing spectra from the 1.3 μm band to the 1.5 μm band is desirable for larger circuit bandwidth and functionality.

In this work, we demonstrate room-temperature in-plane InP/InGaAs nano-laser array epitaxially grown on (001) SOI substrates emitting at the 1.5 μm band. Starting with InP/InGaAs nano-ridges selectively grown inside nano-scale Si trenches on SOI, we achieve strong on-chip mode confinement by designing air-surrounded nano-cavities supported by partially-etched Si pedestals, and thus obtain room temperature stimulated emission under optical excitation. More significantly, the lasing peak can be tuned to cover the E band, the S band and the C band through selection of the nano-cavity length defined by lithography. Compared with our previous transferred InP/InGaAs nano-ridge lasers with random orientations [19], the monolithic integration of well-aligned telecom nano-lasers on (001) SOI wafers using selective area hetero-epitaxy combined with traditional top-down processing offers an intriguing path towards compact on-chip III-V light sources for Si photonics.

Fig. 1(a) schematically delineates the designed InP/InGaAs nano-laser array directly grown on (001) SOI. We adopted conventional Fabry-Perot (FP) cavity with etched end-facets to examine the feasibility of our design. The in-plane InP/InGaAs nano-lasers are underpinned by Si pedestals with a triangular-shaped cross-section, the size of which is carefully controlled to ensure a strong mode confinement inside the nano-ridge as well as robust mechanical support for the top laser cavity. Note that, the supporting Si pedestal with atomic sharp {111} surfaces also serves as a low-loss waveguide to couple light out from the above laser cavity, providing potential on-chip light manipulation. The fabrication process is briefly outlined in Fig. 1(b). Starting with InP/InGaAs nano-ridges grown on SOI substrates, the oxide spacers were selectively etched away using buffered oxide etch. Then, aiming at minimizing light loss into the Si device layer, the underneath Si was undercut to a triangular-shaped post using potassium hydroxide based selective wet etch. In the next step, an oxide layer with a thickness of 300 nm was deposited onto the sample using plasma enhanced chemical vapor deposition (PECVD). This PECVD oxide provides a uniform coverage of the nano-ridges and the Si pedestals, and serves as a protection mask during the subsequent etching process. Finally, the end-facets of nano-laser cavities with different lengths were defined using focused ion beam milling (FIB), and the oxide mask was selectively removed using buffered oxide etch afterwards. Note that the nano-laser array demonstrated here could also be easily fabricated using traditional photolithography and dry etching process with other dimensions and thus by no means compromises their co-integration with other Si based optical elements.

The InP/InGaAs nano-ridges in this experiment were grown on (001) SOI substrates to ensure a strong on-chip mode confinement inside the as-grown nano-ridges and compatibility with the current Si photonics platform. We started with commercial 4-inch (001) SOI wafers with a 2.0 ± 0.5 μm thick Si device layer, a 1.0 μm thick buried oxide layer and a 500 μm thick Si handle layer. To reduce light leakage into the underlying Si device layer and confine light within the epitaxial III-V alloy, the SOI layer was thinned down to around 600 nm using cycled thermal oxidation and subsequent buffered oxide etch process [20]. Then [110] oriented SiO_2 stripes, with a line pitch of 2.8 μm, a trench opening of 450 nm and a trench length of 15 mm, were defined atop the Si device layer. The large separation of adjacent trenches ensures minimal light coupling between neighboring nano-ridges to allow for probing of the optical properties of individual nano-cavities. After patterning, we grew InP/InGaAs nano-ridges inside the nano-scale Si trenches using metal organic chemical vapor deposition. A detailed description and development of the hetero-epitaxial process can be found in Ref [21-23]. Fig. 2(a) displays a 70° tilted-view scanning electron microscope (SEM) image of the as-grown sample, showing equally-spaced in-plane InP nano-ridge array inside nano-scale Si trenches. Similar to nano-ridges grown on Si substrates, structures grown on SOI also exhibit a faceted growth front with two convex {111} facets connected by a flat (001) facet [24]. The cross-sectional transmission electron microscope (TEM) photo of one nano-ridge is presented in Fig. 2(b). With a width of 450 nm and a height of 1.0 μm, the nano-ridges could efficiently

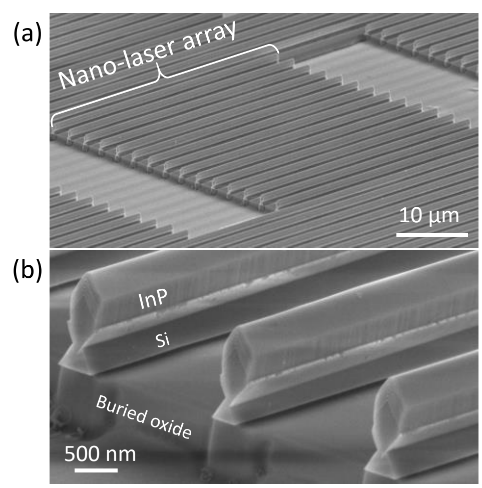

Fig. 3. (a) Tilted-view SEM image of the InP/InGaAs nano-laser array on (001) SOI. (b) Zoomed-in SEM image of the end-facets of the nano-laser array.

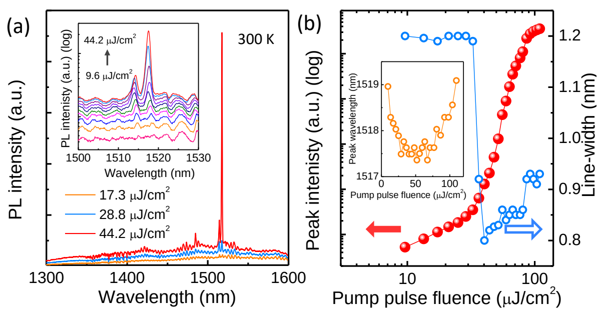

Fig. 4. (a) Room temperature emission spectra around threshold. Inset shows the emission spectra plotted in a logarithmic scale. (b) The evolution of the peak intensity and the line-width as the excitation level increases. Inset presents the progression of peak position as a function of pumping levels.

guide optical modes at the telecom bands [25]. The large lattice mismatch between InP and Si is accommodated through the formation of a thin layer of high-density planar defects at the III-V/Si interface, rendering the upper InP main layer with high crystalline quality. We embedded five In$_{0.53}$Ga$_{0.47}$As ridge quantum wells inside the InP nano-ridge using a "cycled growth procedure" [19], as shown in Fig. 2(d). The atomically-flat {111} facets developed during the selective area growth process result in sharp interfaces between the ridge InGaAs and InP continuum, which in turn minimizes the interfacial non-radiative recombination and maximizes the light emitting efficiency. At room temperature, the as-grown InP/InGaAs nano-ridge array emits around 1500 nm and serves as the gain medium for wavelengths in the E, the S and the C band (see Fig. 2(c)).

Fig. 3(a) displays a tilted-view SEM image of the finalized InP/InGaAs nano-laser array on SOI. The end-facets of the laser cavity were created by etching two parallel trenches with a length of 40 μm, a width of 15 μm and a depth of 2.0 μm. Consequently, each nano-laser array consists of 15 equally-distributed individual nano-lasers. These nano-lasers feature a highly-ordered in-plane configuration with horizontal light emission. A close-up of the end-facets of the InP/InGaAs nano-cavities with the supporting Si pedestals and the buried oxide layer is presented in Fig. 3(b). The morphology of the end-facets defined by FIB is pretty smooth, while the profile exhibits a slight incline towards the nano-ridge tip. These non-vertical profile could in turn result in non-parallel end-facets. However, the influence on the overall round-trip loss should be inconsequential since optical feedback of the end-facets comes from scattering instead of direct reflection because of the sub-wavelength dimension [26]. The size of the supporting Si pedestals also exhibits a variation, which could influence the mode distribution inside the nano-cavity and accordingly affect the propagation loss and the modal gain. The fluctuation of the pedestal size results from the thickness variation of the initial SOI wafers, and a more uniform nano-laser array can be readily achieved using SOI substrates with better uniformity.

The on-chip nano-lasers were characterized at room temperature using a home-built micro-photoluminescence system and laser oscillation was achieved under optical pumping by a mode-locked Ti/Sapphire laser (750 nm, 100 fs pulses and a repetition rate of 76 MHz). The excitation laser beam was focused into a line-shaped spot by a cylindrical lens to cover the entire nano-cavity. Fig. 4(a) provides the emission spectra of one nano-laser with a length of 60 μm measured under different pumping fluences. At low pumping levels, the probed nano-laser features a broad spontaneous emission and well-spaced FP resonance peaks. As the pumping level increases, the peak at 1518 nm amplifies, protrudes from the background emission, and finally lases. The lasing behavior is further attested by the clamping of spontaneous emission around threshold, as shown by the emission spectra plotted in a logarithmic scale (see the inset of Fig. 4(a)). Single-mode lasing is achieved, albeit the adoption of simple FP cavity. Fig. 4(b) displays the evolution of the peak intensity and the line-width at 1518 nm as a function of the excitation levels. A clear S-shape is detected from the L-L curve, and a lasing threshold around 40 μJ/cm^2 is extracted. This value is about double of that of the transferred nano-lasers (smaller than 20 μJ/cm^2) [19]. We attribute the somewhat larger lasing thresholds of nano-lasers on SOI to the supporting Si pedestals which leads to a reduced modal gain. Far above threshold, the intensity of the single lasing mode at 1518 nm is orders of magnitudes higher than the clamped background emission, and a few weak side modes start to appear at the blue side. The line-width of the lasing peak narrows from 1.2 nm to 0.8 nm around threshold, and then gradually augments to 0.9 nm as the excitation levels continues to increase. The subsequent broadening of the line-width above threshold could be ascribed to wavelength chirp, where the fluctuation of carrier density induces the variation of refractive index [10, 13, 16]. The inset of Fig. 4(b) summarizes the progression of the peak position as the pumping level strengthens. The lasing mode initially blue-shifts below threshold, then saturates around 1517.5 nm around threshold, and finally red-shifts above threshold. The variation of the peak position is directly modulated by the alteration of refractive index. Three different mechanisms, namely band-filling effects, band-gap shrinkage and free-carrier absorption, contribute to carrier-induced change of refractive

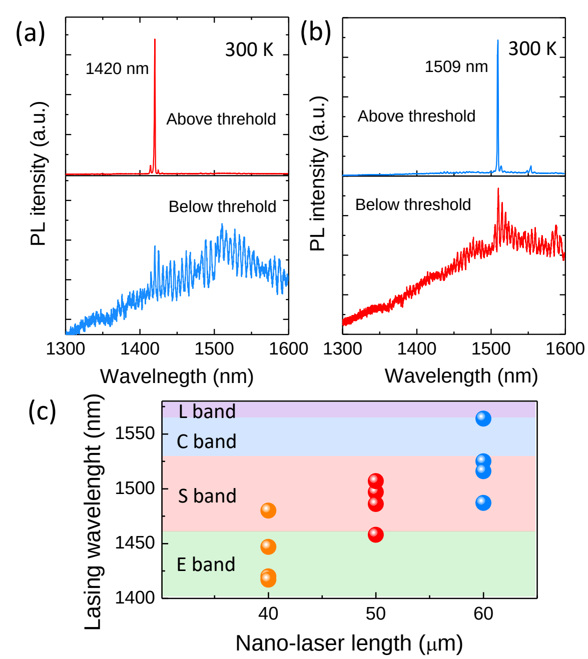

Fig. 5. (a) PL spectra of one nano-laser with a length of 40 μm measured below and above threshold. (b) PL spectra of one nano-laser with a length of 50 μm measured below and above threshold. (c) The relationship of the lasing peak and the length of the nano-cavity.

index. For InP based materials and a mode wavelength of 1.5 μm, the combination effect results in a reduced refractive index [27], which consequently causes the initial blue-shift of the lasing peak. As the excitation level escalates and the nano-laser heats up, another effect called "thermal-induced change of refractive index" comes into play and leads to an increased refractive index [28]. The synergized effect of carrier-induced and thermal-induced changes of refractive index brings on the saturation and following red-shift of the lasing peak.

We also observed room-temperature lasing behavior from nano-lasers with different cavity lengths. Fig. 5(a) displays the measured photoluminescence spectra of one nano-laser with a length of 40 μm. Below threshold, we detect a broad spontaneous emission centered around 1.5 μm, modulated by evenly-spaced FP longitudinal modes. The mode spacing around 1.5 μm is extracted as 5.7 nm corresponding to a group refractive index of 4.9. Above threshold, single-mode lasing is obtained at 1420 nm. The measured emission spectra of one nano-laser with a length of 50 μm is presented in Fig. 5(b). As expected, the spacing between adjacent longitudinal modes reduces to 4.5 nm. Interestingly, the lasing peak also red-shifts to 1509 nm. Fig. 5(c) summarizes the relationship of the lasing mode and the nano-laser length. Similar to the phenomenon observed from transferred nano-lasers [19], the lasing wavelength of nano-lasers grown on SOI exhibits a strong dependence on the length of the nano-cavity, with a longer nano-cavity corresponding to a larger emission wavelength. The correlation between the lasing mode and the cavity length might stem from the wavelength-dependent modal gain and propagation/end-facet loss. A longer mode wavelength features a larger round-trip loss and a smaller modal gain, and thereby necessitates a larger volume of active material to reach threshold. We will fabricate more nano-lasers with a wider length variation to investigate the detailed mechanism.

In conclusion, we have demonstrated room temperature InP/InGaAs nano-laser arrays monolithically integrated on (001) SOI substrate emitting at the telecom bands. Room temperature laser oscillation corroborates the excellent optical quality of III-V nano-ridges directly grown on Si, and affirms the validity of our proposed laser design. Incorporating in-plane nano-laser array with Si-transparent light emission onto CMOS-compatible (001) SOI substrates suggests the feasibility of on-chip consolidation between compact III-V light sources and mature Si photonic components. Future work includes operating the nano-lasers under continuous-wave excitation via advanced cavity designs, and realization of electrically driven telecom InP/InGaAs nano-laser arrays on (001) SOI.

Funding. Research Grants Council of Hong Kong (16245216, 16212115 and AoE/P-02/12); Innovation Technology Fund of Hong Kong (ITS/273/16FP); William Mong Institute of Nano Science and Technology (WMINST19/SC04).

Acknowledgement. The authors would like to thank the MCPF and NFF of HKUST for technical support. Helpful discussion with C. W. Tang is also acknowledged.

References

1. Thomson, David, Aaron Zilkie, John E. Bowers, Tin Komljenovic, Graham T. Reed, Laurent Vivien, Delphine Marris-Morini. Journal of Optics 18, no. 7 (2016): 073003.
2. Liang, Di, and John E. Bowers. Nature photonics 4, no. 8 (2010): 511.
3. Zhou, Zhiping, Bing Yin, and Jurgen Michel. Light: Science & Applications 4, no. 11 (2015): e358.
4. Wang, Zhechao, Amin Abbasi, Utsav Dave, Andreas De Groote, Sulakshna Kumari, Bernadette Kunert, Clement Merckling et al Laser & Photonics Reviews 11, no. 4 (2017): 1700063.
5. Chen, Siming, Wei Li, Jiang Wu, Qi Jiang, Mingchu Tang, Samuel Shutts, Stella N. Elliott et al. Nature Photonics 10, no. 5 (2016): 307.
6. Liu, Alan Y., Chong Zhang, Justin Norman, Andrew Snyder, Dmitri Lubyshev, Joel M. Fastenau, Amy WK Liu, Arthur C. Gossard, and John E. Bowers. Applied Physics Letters 104, no. 4 (2014): 041104.
7. Wan, Yating, Justin Norman, Qiang Li, M. J. Kennedy, Di Liang, Chong Zhang, Duanni Huang et al. Optica 4, no. 8 (2017): 940-944.
8. Yan, Ruoxue, Daniel Gargas, and Peidong Yang. Nature photonics 3, no. 10 (2009): 569.
9. Saxena, Dhruv, Sudha Mokkapati, Patrick Parkinson, Nian Jiang, Qiang Gao, Hark Hoe Tan, and Chennupati Jagadish. Nature Photonics 7, no. 12 (2013): 963.
10. Tatebayashi, Jun, Satoshi Kako, Jinfa Ho, Yasutomo Ota, Satoshi Iwamoto, and Yasuhiko Arakawa. Nature Photonics 9, no. 8 (2015): 501.
11. Chen, Roger, Thai-Truong D. Tran, Kar Wei Ng, Wai Son Ko, Linus C. Chuang, Forrest G. Sedgwick, and Connie Chang-Hasnain. Nature Photonics 5, no. 3 (2011): 170.
12. Mayer, B., L. Janker, B. Loitsch, J. Treu, T. Kostenbader, S. Lichtmannecker, T. Reichert et al Nano letters 16, no. 1 (2015): 152-156.
13. Kim, Hyunseok, Wook-Jae Lee, Alan C. Farrell, Juan SD Morales, Pradeep Senanayake, Sergey V. Prikhodko, Tomasz J. Ochalski, and Diana L. HuffakerNano letters 17, no. 6 (2017): 3465-3470.
14. Lu, Fanglu, Indrasen Bhattacharya, Hao Sun, Thai-Truong D. Tran, Kar Wei Ng, Gilliard N. Malheiros-Silveira, and Connie Chang-Hasnain. Optica 4, no. 7 (2017): 717-723.
15. Kim, Hyunseok, Wook-Jae Lee, Alan C. Farrell, Akshay Balgarkashi, and Diana L. Huffaker. Nano letters 17, no. 9 (2017): 5244-5250.
16. Wang, Zhechao, Bin Tian, Marianna Pantouvaki, Weiming Guo, Philippe Absil, Joris Van Campenhout, Clement Merckling, and Dries Van Thourhout. Nature Photonics 9, no. 12 (2015): 837.
17. Tian, Bin, Zhechao Wang, Marianna Pantouvaki, Philippe Absil, Joris Van Campenhout, Clement Merckling, and Dries Van Thourhout. Nano letters 17, no. 1 (2016): 559-564.
18. Shi, Yuting, Zhechao Wang, Joris Van Campenhout, Marianna Pantouvaki, Weiming Guo, Bernardette Kunert, and Dries Van Thourhout Optica 4, no. 12 (2017): 1468-1473.
19. Han, Yu, Wai Kit Ng, Chao Ma, Qiang Li, Si Zhu, Christopher CS Chan, Kar Wei Ng et al. Optica 5, no. 8 (2018): 918-923.
20. Kim, Hyunseok, Alan C. Farrell, Pradeep Senanayake, Wook-Jae Lee, and Diana L. Huffaker. Nano letters 16, no. 3 (2016): 1833-1839.
21. Han, Yu, Qiang Li, Shih-Pang Chang, Wen-Da Hsu, and Kei May Lau. Applied Physics Letters 108, no. 24 (2016): 242105.
22. Han, Yu, Qiang Li, and Kei May Lau. Journal of Applied Physics 120, no. 24 (2016): 245701.
23. Han, Yu, Qiang Li, Kar Wei Ng, Si Zhu, and Kei May Lau. Nanotechnology 29, no. 22 (2018): 225601.
24. Biasiol, G., Anders Gustafsson, K. Leifer, and E. Kapon. Physical Review B 65, no. 20 (2002): 205306.
25. Han, Yu, Qiang Li, Si Zhu, Kar Wei Ng, and Kei May Lau. Applied Physics Letters 111, no. 21 (2017): 212101.
26. Zimmler, Mariano A., Federico Capasso, Sven Müller, and Carsten Ronning. Semiconductor Science and Technology 25, no. 2 (2010): 024001.
27. Bennett, Brian R., Richard A. Soref, and Jesus A. Del Alamo. IEEE Journal of Quantum Electronics 26, no. 1 (1990): 113-122.
28. McCaulley, J. A., V. M. Donnelly, M. Vernon, and I. Taha. Physical Review B 49, no. 11 (1994): 7408.

Full References

1. Thomson, David, Aaron Zilkie, John E. Bowers, Tin Komljenovic, Graham T. Reed, Laurent Vivien, Delphine Marris-Morini et al. "Roadmap on silicon photonics." Journal of Optics 18, no. 7 (2016): 073003.
2. Liang, Di, and John E. Bowers. "Recent progress in lasers on silicon." Nature photonics 4, no. 8 (2010): 511.
3. Zhou, Zhiping, Bing Yin, and Jurgen Michel. "On-chip light sources for silicon photonics." Light: Science & Applications 4, no. 11 (2015): e358.
4. Wang, Zhechao, Amin Abbasi, Utsav Dave, Andreas De Groote, Sulakshna Kumari, Bernadette Kunert, Clement Merckling et al. "Novel light source integration approaches for silicon photonics." Laser & Photonics Reviews 11, no. 4 (2017): 1700063.
5. Chen, Siming, Wei Li, Jiang Wu, Qi Jiang, Mingchu Tang, Samuel Shutts, Stella N. Elliott et al. "Electrically pumped continuous-wave III–V quantum dot lasers on silicon." Nature Photonics 10, no. 5 (2016): 307.
6. Liu, Alan Y., Chong Zhang, Justin Norman, Andrew Snyder, Dmitri Lubyshev, Joel M. Fastenau, Amy WK Liu, Arthur C. Gossard, and John E. Bowers. "High performance continuous wave 1.3 μ m quantum dot lasers on silicon." Applied Physics Letters 104, no. 4 (2014): 041104.
7. Wan, Yating, Justin Norman, Qiang Li, M. J. Kennedy, Di Liang, Chong Zhang, Duanni Huang et al. "1.3 μm submilliamp threshold quantum dot micro-lasers on Si." Optica 4, no. 8 (2017): 940-944.
8. Yan, Ruoxue, Daniel Gargas, and Peidong Yang. "Nanowire photonics." Nature photonics 3, no. 10 (2009): 569.
9. Saxena, Dhruv, Sudha Mokkapati, Patrick Parkinson, Nian Jiang, Qiang Gao, Hark Hoe Tan, and Chennupati Jagadish. "Optically pumped room-temperature GaAs nanowire lasers." Nature Photonics 7, no. 12 (2013): 963.
10. Tatebayashi, Jun, Satoshi Kako, Jinfa Ho, Yasutomo Ota, Satoshi Iwamoto, and Yasuhiko Arakawa. "Room-temperature lasing in a single nanowire with quantum dots." Nature Photonics 9, no. 8 (2015): 501.
11. Chen, Roger, Thai-Truong D. Tran, Kar Wei Ng, Wai Son Ko, Linus C. Chuang, Forrest G. Sedgwick, and Connie Chang-Hasnain. "Nanolasers grown on silicon." Nature Photonics 5, no. 3 (2011): 170.
12. Mayer, B., L. Janker, B. Loitsch, J. Treu, T. Kostenbader, S. Lichtmannecker, T. Reichert et al. "Monolithically integrated high-β nanowire lasers on silicon." Nano letters 16, no. 1 (2015): 152-156.
13. Kim, Hyunseok, Wook-Jae Lee, Alan C. Farrell, Juan SD Morales, Pradeep Senanayake, Sergey V. Prikhodko, Tomasz J. Ochalski, and Diana L. Huffaker. "Monolithic InGaAs nanowire array lasers on silicon-on-insulator operating at room temperature." Nano letters 17, no. 6 (2017): 3465-3470.
14. Lu, Fanglu, Indrasen Bhattacharya, Hao Sun, Thai-Truong D. Tran, Kar Wei Ng, Gilliard N. Malheiros-Silveira, and Connie Chang-Hasnain. "Nanopillar quantum well lasers directly grown on silicon and emitting at silicon-transparent wavelengths." Optica 4, no. 7 (2017): 717-723.
15. Kim, Hyunseok, Wook-Jae Lee, Alan C. Farrell, Akshay Balgarkashi, and Diana L. Huffaker. "Telecom-wavelength bottom-up nanobeam lasers on silicon-on-insulator." Nano letters 17, no. 9 (2017): 5244-5250.
16. Wang, Zhechao, Bin Tian, Marianna Pantouvaki, Weiming Guo, Philippe Absil, Joris Van Campenhout, Clement Merckling, and Dries Van Thourhout. "Room-temperature InP distributed feedback laser array directly grown on silicon." Nature Photonics 9, no. 12 (2015): 837.
17. Tian, Bin, Zhechao Wang, Marianna Pantouvaki, Philippe Absil, Joris Van Campenhout, Clement Merckling, and Dries Van Thourhout. "Room temperature O-band DFB laser array directly grown on (001) silicon." Nano letters 17, no. 1 (2016): 559-564.
18. Shi, Yuting, Zhechao Wang, Joris Van Campenhout, Marianna Pantouvaki, Weiming Guo, Bernardette Kunert, and Dries Van Thourhout. "Optical pumped InGaAs/GaAs nano-ridge laser epitaxially grown on a standard 300-mm Si wafer." Optica 4, no. 12 (2017): 1468-1473.
19. Han, Yu, Wai Kit Ng, Chao Ma, Qiang Li, Si Zhu, Christopher CS Chan, Kar Wei Ng et al. "Room-temperature InP/InGaAs nano-ridge lasers grown on Si and emitting at telecom bands." Optica 5, no. 8 (2018): 918-923.
20. Kim, Hyunseok, Alan C. Farrell, Pradeep Senanayake, Wook-Jae Lee, and Diana L. Huffaker. "Monolithically integrated InGaAs nanowires on 3D structured silicon-on-insulator as a new platform for full optical links." Nano letters 16, no. 3 (2016): 1833-1839.
21. Han, Yu, Qiang Li, Shih-Pang Chang, Wen-Da Hsu, and Kei May Lau. "Growing InGaAs quasi-quantum wires inside semi-rhombic shaped planar InP nanowires on exact (001) silicon." Applied Physics Letters 108, no. 24 (2016): 242105.
22. Han, Yu, Qiang Li, and Kei May Lau. "Highly ordered horizontal indium gallium arsenide/indium phosphide multi-quantum-well in wire structure on (001) silicon substrates." Journal of Applied Physics 120, no. 24 (2016): 245701.
23. Han, Yu, Qiang Li, Kar Wei Ng, Si Zhu, and Kei May Lau. "InGaAs/InP quantum wires grown on silicon with adjustable emission wavelength at telecom bands." Nanotechnology 29, no. 22 (2018): 225601.
24. Biasiol, G., Anders Gustafsson, K. Leifer, and E. Kapon. "Mechanisms of self-ordering in nonplanar epitaxy of semiconductor nanostructures." Physical Review B 65, no. 20 (2002): 205306.
25. Han, Yu, Qiang Li, Si Zhu, Kar Wei Ng, and Kei May Lau. "Continuous-wave lasing from InP/InGaAs nanoridges at telecommunication wavelengths." Applied Physics Letters 111, no. 21 (2017): 212101.
26. Zimmler, Mariano A., Federico Capasso, Sven Müller, and Carsten Ronning. "Optically pumped nanowire lasers: invited review." Semiconductor Science and Technology 25, no. 2 (2010): 024001.
27. Bennett, Brian R., Richard A. Soref, and Jesus A. Del Alamo. "Carrier-induced change in refractive index of InP, GaAs and InGaAsP." IEEE Journal of Quantum Electronics 26, no. 1 (1990): 113-122.
28. McCaulley, J. A., V. M. Donnelly, M. Vernon, and I. Taha. "Temperature dependence of the near-infrared refractive index of silicon, gallium arsenide, and indium phosphide." Physical Review B 49, no. 11 (1994): 7408.